



**HAL**  
open science

# Determination of the linewidth enhancement factor of semiconductor lasers by complete optical field reconstruction

Brian Siquin, Marco Romanelli

► **To cite this version:**

Brian Siquin, Marco Romanelli. Determination of the linewidth enhancement factor of semiconductor lasers by complete optical field reconstruction. *Optics Letters*, 2023, 48 (4), pp.863-866. 10.1364/ol.483776 . hal-03940670

**HAL Id: hal-03940670**

**<https://hal.science/hal-03940670>**

Submitted on 31 Jan 2023

**HAL** is a multi-disciplinary open access archive for the deposit and dissemination of scientific research documents, whether they are published or not. The documents may come from teaching and research institutions in France or abroad, or from public or private research centers.

L'archive ouverte pluridisciplinaire **HAL**, est destinée au dépôt et à la diffusion de documents scientifiques de niveau recherche, publiés ou non, émanant des établissements d'enseignement et de recherche français ou étrangers, des laboratoires publics ou privés.



Distributed under a Creative Commons Attribution 4.0 International License

# Determination of the linewidth enhancement factor of semiconductor lasers by complete optical field reconstruction

BRIAN SINQUIN<sup>id</sup>, MARCO ROMANELLI<sup>id</sup>

Institut FOTON, UMR 6082, Univ. Rennes 1, 35000 Rennes, France

[brian.sinquin@univ-rennes1.fr](mailto:brian.sinquin@univ-rennes1.fr)

January 21, 2023

## Abstract

*We show that the method of complete optical field reconstruction introduced in [Opt. Lett. 23, 1784 (1998)] allows a precise determination of the linewidth enhancement factor (LEF) of semiconductor lasers. We determine experimentally the LEF with 3 % uncertainty. The method is rather simple and reliable, and is of interest in the context of microwave photonics. While particularly adapted to actively modulated devices, the proposed approach can in principle be applied to any laser exhibiting a time-periodic behaviour.*

Several important applications, such as high-speed data telecommunication systems [1], direct-modulation optoelectronic oscillators [2, 3], or optical sampling with gain-switched pulses [4], require operating semiconductor lasers under high-frequency modulation of the pump current. A crucial parameter to model and predict the behaviour of semiconductor lasers under such operating conditions is the linewidth enhancement factor (LEF), typically indicated as  $\alpha$  [5]. LEF quantifies the relation of phase fluctuations to intensity fluctuations, and plays an important role in many effects, such as linewidth enhancement, frequency chirp during pulsed operation, sensitivity to optical feedback, etc. [6]. A recent example of its ubiquitous occurrence in semiconductor laser physics is, for instance, its role in quantum-cascade laser frequency combs [7]. A reasonably precise knowledge of the  $\alpha$  value is thus very important for predicting the behaviour of a given laser. The measurement of  $\alpha$  is notoriously quite tricky, and many different methods have been proposed, based on spectral measurements, small or large signal modulation, optical injection or optical feedback, or other. In ref [8], up to 11 different methods are listed, and several references to many of the existing techniques are given also in [9, 10].

On the other hand, specific techniques, adapted to “long” pulses (of the order of tens of ps) with high repetition rates (GHz range) of interest in optical networks, have been developed for the complete characterization of optical fields [11, 12, 13]. These techniques allow reconstructing the temporal variations  $I(t)$  and  $\phi(t)$  of the optical intensity and phase respectively. It has been recognized that, using these methods, one can also extract the LEF with good precision. For instance, Consoli et al. [10] have used the PROUD method of pulse characterization [12] to obtain the LEF of gain-switched DFB lasers and VCSELs. The method introduced in [11], that we will indicate from now on as Debeau’s method, has been recently used to measure the chirp of MZM modulators [14] and of pulses amplified by quantum dash SOAs [15] but, to the best of our knowledge, it has never been applied to the precise determination of the LEF of strongly-modulated semiconductor lasers, even if it is particularly well suited for this situation.

In this paper we show that the Debeau’s method of optical pulse reconstruction is effective for the accurate determination, within a few percents, of the LEF of semiconductor lasers, and therefore represents a valuable alternative to other techniques. Debeau’s method

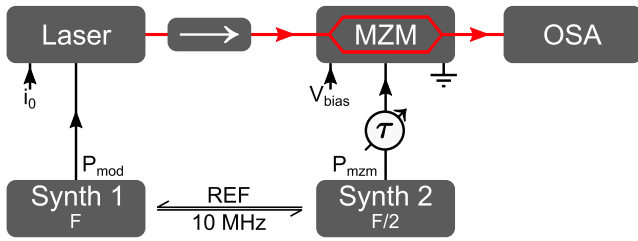


Figure 1: Experimental setup.

is particularly appealing in the context of microwave photonics and of optical generation of radiofrequency waveforms [16], because it requires techniques and equipment typical of this field and can be implemented rather straightforwardly. With respect to [12], Debeau's method has the advantage of relying on spectral measurements, thus avoiding the need of time-resolved measurements of the pulse intensity profile. Furthermore, it is based on relative measurements, and thus does not require cumbersome calibrations. The paper is organized as follows. First we briefly revise, for self-consistency and clarity, Debeau's method [11]. Then, experimental results are presented and discussed.

The principle of the method used for pulse reconstruction is sketched in Fig. 1. It is of rather simple implementation, as it requires high-frequency modulation of the pump current of the laser under study, a Mach-Zehnder modulator (MZM), a RF variable delay line and an optical spectrum analyser (OSA). The principle is as follows. The optical field at the output of the MZM is  $E_{out} = \frac{1}{2}[1 + \exp(i\phi)]E_{in}$ . The MZM is biased at the extinction point and driven by an RF synthesizer at half the repetition frequency  $F$  of the pulse train, so that  $\phi$  reads  $\phi(t) = \pi + \phi_m \cos[2\pi\frac{F}{2}(t - \tau)]$ , where  $\tau$  is controlled by the RF variable delay line.

For a monochromatic input field  $E_{in} = E_0 e^{i\phi_0} e^{i2\pi f_0 t}$  and small modulation amplitude  $\phi_m$  we would get an output field

$$E_{out} = -\frac{i}{4}\phi_m |E_0| e^{i2\pi(f_0 - F/2)t} e^{i(\phi_0 + \pi F\tau)} - \frac{i}{4}\phi_m |E_0| e^{i2\pi(f_0 + F/2)t} e^{i(\phi_0 - \pi F\tau)}, \quad (1)$$

constituted of two spectral lines at frequencies  $f_0 - F/2$  and  $f_0 + F/2$  respectively, with different spectral phases, controlled by the variable delay  $\tau$ .

For a multifrequency input field, the situation is sketched schematically in Fig. 2: the spectrum of the

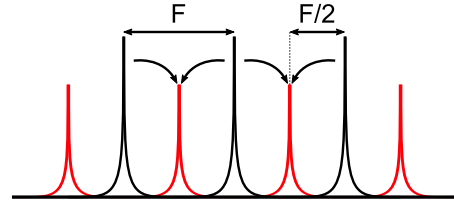


Figure 2: Principle of the method, illustrated for an input field composed of three frequencies separated by  $F$ . The output field exiting from the MZM has in this case two central frequencies, produced by the sidebands interference, carrying the information about spectral phases of the input field.

output field is composed of lines separated by  $F$ , and each of these lines (except the first and the last) is the superposition of two sidebands originating from two consecutive lines of the input spectrum.

For an input field  $E_{in}(t)$  in the form:

$$E_{in}(t) = \sum_{k=0}^N |E_k| e^{i\phi_k} e^{i2\pi(f_0 + kF)t}, \quad (2)$$

with  $f_0$  being the lowest frequency in the input spectrum, the output of the MZM can be written, by making use of eq. 1 for each frequency component and rearranging the terms:

$$E_{out} = |E_0| e^{i2\pi(f_0 - F/2)t} e^{i(\phi_0 + \pi F\tau)} + \sum_{k=0}^{N-1} \left[ |E_k| e^{i(\phi_k - \pi F\tau)} + |E_{k+1}| e^{i(\phi_{k+1} + \pi F\tau)} \right] e^{i2\pi(f_0 + kF + F/2)t} + |E_N| e^{i2\pi(f_0 + NF + F/2)t} e^{i(\phi_N - \pi F\tau)}. \quad (3)$$

It results that, ignoring the extreme lines at  $f_0 - F/2$  and at  $f_0 + NF + F/2$ , the output field can be written as

$$E_{out} = \sum_{k=0}^{N-1} B(k, \tau) e^{i2\pi(f_0 + kF + F/2)t}. \quad (4)$$

The power of the frequency component  $f_0 + kF + F/2$  of the spectrum of  $E_{out}$  is thus

$$|B(k, \tau)|^2 = |E_k|^2 + |E_{k+1}|^2 + 2|E_k||E_{k+1}| \cos(\phi_{k+1} - \phi_k + 2\pi F\tau). \quad (5)$$

Eq. 5 is the cornerstone of the Debeau's method. Each coefficient  $|B(k, \tau)|^2$  is expected to display a sinusoidal variation when the RF delay  $\tau$  is changed. From such variation the spectral phase differences  $\phi_{k+1} - \phi_k$  can be inferred. Proceeding recursively, all the phases  $\phi_k$  can be obtained, with the phase  $\phi_0$  of the first line taken as a reference. Since the spectral powers  $|E_k|^2$  are easily measured with a high-resolution OSA, one has a complete knowledge of the spectral amplitudes and phases, from which one can reconstruct the time-domain behaviour  $E_{in}(t)$  using Eq. 2.

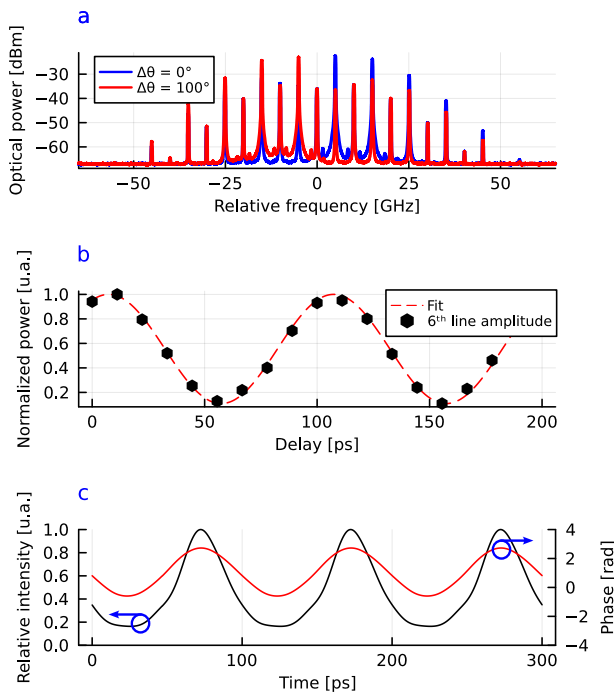


**Figure 3:** (a) Recorded optical spectra for  $\Delta\theta = 2\pi F\tau = 0^\circ$  and  $100^\circ$  respectively. (b) Power of the 6<sup>th</sup> spectral line  $|B(5, \tau)|^2$  plotted as a function of  $\tau$ . (c) Reconstructed time traces of the intensity  $I(t)$  and phase  $\phi(t)$ .

We apply the above method to a InGaAsP/InAs DFB laser (Gooch & Housego, AA0701) emitting at  $1.55 \mu\text{m}$ . The bias current and the temperature of the laser are set using a laser diode controller (ILX Lightwave LDC-3900). A strong modulation at 10 GHz, provided by a RF synthesizer (Rohde & Schwartz SMF 100A), is added to the laser bias current through an internal bias-tee. A second RF synthesizer (Rohde & Schwartz SMB 100A), whose internal 10 MHz clock is phase-

locked to the first one, drives a LiNbO<sub>3</sub> MZM (ixblue Photonics MXAN-LN-10) at half the pulse repetition frequency. A variable RF delay is introduced using a coaxial phase-shifter (Narda model 3752,  $4^\circ/\text{GHz}$ ). The optical spectrum is then measured with a high-resolution OSA (Apex Technologies AP2083A) using a resolution bandwidth (RBW) of 400 MHz. This value of the RBW results from a compromise between the need of separating the spectral lines, and the need of integrating over the fluctuations of the optical frequency of the laser. The MZM is driven at a power  $P_{mzm} = 4.5 \text{ dBm}$  in order to fulfill the low modulation criterion that permits to use Eq. 1. This corresponds to  $\phi_m = \pi \frac{\sqrt{2RP_{mzm}}}{V_\pi} = 0.28 \ll 2\pi$  with  $V_\pi = 6 \text{ V}$ . To illustrate the method, we drive the laser with a DC current of  $i_0 = 39 \text{ mA}$  and a RF modulation power of  $P_{mod} = 12.8 \text{ dBm}$  at a frequency of 10 GHz.

Two experimentally recorded optical spectra, such that the phase delay  $\Delta\theta = 2\pi F\tau$  is equal to  $0^\circ$  and  $100^\circ$  respectively are shown in Fig. 3 (a). It is apparent that the amplitudes of the spectral lines varies with  $\theta$ , because of the interference of the two sidebands originating from different spectral lines of the input field. Fig. 3 (b) shows  $|B(k, \tau)|^2$  as a function of the delay for a particular line. The sinusoidal variation expected from Eq. 5 is well verified and a fit allows retrieving the corresponding initial phase, i.e. the spectral phase difference  $\phi_{k+1} - \phi_k$ . Doing the same for all the spectral lines, we are able to retrieve all the spectral phases, and to reconstruct the time variations of  $I(t)$  and  $\phi(t)$  shown in Fig. 3 (c).

Once the complete characterization of the optical field is available, we are able to deduce the phase-amplitude coupling in the laser. To do so, we assume that  $I$  and  $\phi$  satisfy the standard rate equations [17]

$$\frac{dI}{dt} = NI \quad (6)$$

$$\frac{d\phi}{dt} = \frac{1}{2}\alpha N \quad (7)$$

$$\frac{dN}{dt} = \epsilon [J(t) - 1 - N - (1 + N)I], \quad (8)$$

where  $N$  is the population inversion,  $J(t)$  the pump parameter,  $\epsilon = \frac{\tau_I}{\tau_N}$  the ratio of the cavity and population lifetimes, and time  $t$  is in units of  $\tau_I$ . Under pump current modulation,  $J(t)$  is expressed as follows:

$$J(t) = r(1 + m \cos(2\pi Ft)), \quad (9)$$

with  $r = i_0/i_{th}$  being the bias current normalized to

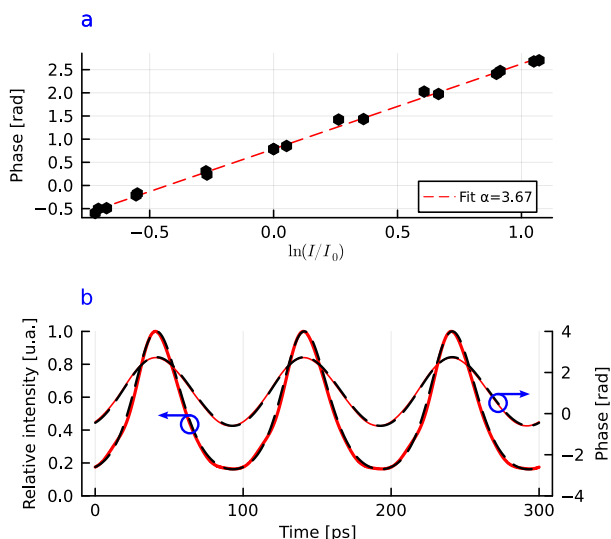


**Figure 4:** (a)  $\phi(t)$  plotted as a function of  $\log(I(t))$ . (b) Reconstructed (full lines) vs simulated (dashed lines)  $I(t)$  and  $\phi(t)$ . The simulation uses eqs. (6-8), with  $\alpha = 3.67$ ,  $r = 3$ ,  $m = 0.59$ ,  $\epsilon = 0.028$ .

threshold and  $m = \frac{1}{i_0} \sqrt{2P_{mod}/R_{las}}$  the modulation index with  $R_{las} = 71\Omega$ . If  $J(t) < 0$ , we set  $J(t) = 0$ , as the laser behaves like a diode when a reverse voltage is applied. From equations (6-7) it follows

$$\frac{d\phi}{dI} = \frac{\alpha}{2I} \implies \phi(t) = \phi_0 + \frac{\alpha}{2} \ln\left(\frac{I(t)}{I_0}\right). \quad (10)$$

This result is checked in Fig. 4 (a). Since the reconstruction is performed measuring 9 spectral lines, we have sampled 17 points, equally spaced in time, from the reconstructed time traces of Fig. 4 (b). In general, if  $N+1$  spectral lines are measured, then the largest accessible frequency component in the Fourier expansion of  $I(t)$  and  $\phi(t)$  is  $f_{max} = NF$ , according to Eq. 2. In the time domain this implies, as a consequence of the Nyquist-Shannon theorem, that the sampling time that must be strictly lower than  $\frac{1}{2NF}$ , i.e. that one must sample more than  $2N$  points per period to reconstruct correctly the waveform. It is seen that the reconstructed  $\phi(t)$  is indeed proportional to  $\ln(I(t))$ . This allows extracting a value for the LEF with good precision:  $\alpha = 3.67 \pm 0.19$ . Here 0.19 is equal to  $2\sigma$ , i.e. the standard deviation at 95% confidence interval [18]. When this value is plugged in the rate equations (6-8), the calculated time-domain variations for  $I(t)$  and  $\phi(t)$

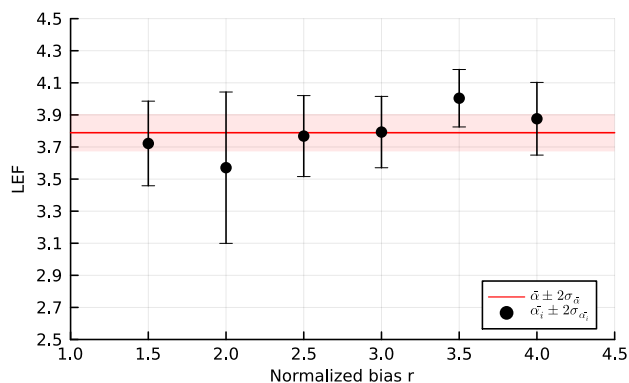


**Figure 5:** Measured values of the LEF as a function of the normalized bias current  $r$ .

are in good agreement with the reconstructed ones (Fig. 4 (b)). Thus, the assumption that the modeling expressed by eqs. (6-8) is accurate enough to capture precisely the laser dynamics is also validated, at least under the operating conditions of the experiment. In particular, we have verified that the inclusion of an extra term in eq. 7 to account for adiabatic chirp [19] is not necessary in our working conditions. The lifetimes  $\tau_I = 5$  ps and  $\tau_N = 180$  ps used in the simulations have been deduced from an independent measurement of the laser transfer function [20]. Having checked the consistency of the method, we have proceeded to a systematic series of measurements for different values of the pump factor  $r$  ( $r = 1$  corresponds to the laser threshold  $i_{th} = 13$  mA) and with a constant RF modulation power  $P_{mod} = 12.8$  dBm. For each value of  $r$ , we have done 10 measurements, on different days, to check the long-term reproducibility of the results. It turns out that it is important to make sure that the MZM is always correctly biased at the extinction point. The MZM we used was subject to small drifts of the bias voltage, presumably due to thermal effects, that could sensibly affect the results if not corrected. The use of a MZM with active bias control should enhance the overall stability of the experiment and, thus, the precision of the final LEF estimation.

The results of the measurements are shown in Fig. 5. The LEF does not seem to exhibit any clear trend with respect to  $r$ . These results are consistent with a constant  $\alpha$  factor, whose value taking into account all the measurements is  $\alpha = 3.79 \pm 0.12$ , where 0.12 is the standard deviation of the mean (SDM) at 95% confi-

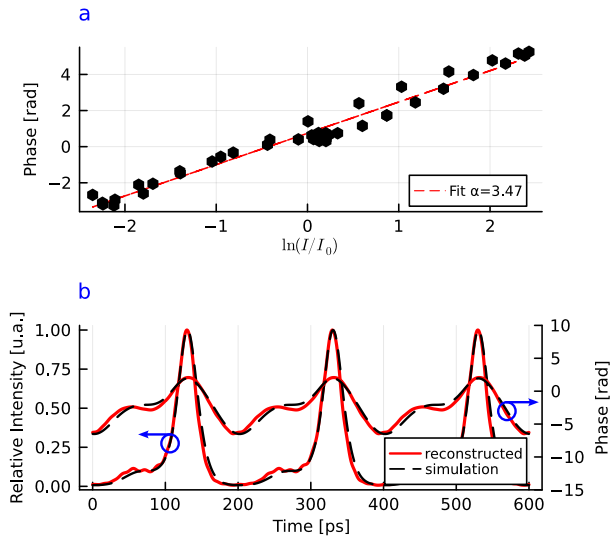


**Figure 6:** (a)  $\phi(t)$  plotted as a function of  $\ln(I(t))$ , for  $i_0 = 26$  mA ( $r = 2$ ). (b) Reconstructed (full lines) vs simulated (dashed lines)  $I(t)$  and  $\phi(t)$ . The simulation uses eqs. (6-8), with  $\alpha = 3.47$ ,  $r = 2$ ,  $m = 1.5$ ,  $\epsilon = 0.028$ .

dence [18], i.e. a relative uncertainty of 3%. In order to have an independent check of our results, we have also measured  $\alpha$  implementing a different method, based on small-signal modulation and on the use of a Mach-Zehnder interferometer as an optical discriminator [9]. In this case we measured the LEF for 12 different values of  $r$  and found  $\alpha = 4.02 \pm 0.11$ . The two results are consistent (and may be combined to further refine the estimate for  $\alpha$ , giving  $\alpha = 3.91 \pm 0.08$ ).

In Fig. 5, it can be noticed that the SDM of the measurement at  $r = 2$  is larger than at other points. This may be caused by the fact that, for  $r = 2$ , we encounter a dynamical instability leading to period doubling [21]. We speculate that, close to the instability threshold, the pulse train may have a significant timing jitter, affecting the precise determination of the spectral phases. A more careful characterization would be needed to precisely elucidate this point. However, the proposed method works quite well also when the gain-switching regime is accompanied by the period-doubling instability. In this case, the pulse repetition frequency is 5 GHz, so that the MZM is driven at 2.5 GHz.

From Fig. 6.a, one can see that, as in Fig. 4.a, the reconstructed temporal phase  $\phi(t)$  is proportional to  $\ln(I(t))$ . There are more points than in Fig. 4.a because

the optical spectrum is broader. The extracted value of the LEF is  $\alpha = 3.47 \pm 0.13$ . When this value is inserted in eqs. (6-8) we again find, in this specific case, a good agreement between the model and the reconstructed signal in Fig. 6.b.

In summary, we have shown that the pulse measurement method introduced in [11] allows a precise determination of the  $\alpha$  factor of a semiconductor laser. The method is robust and of rather simple implementation, and particularly appealing in the context of microwave photonics. We could measure  $\alpha$  with a relative uncertainty of 3%. One advantage of this method is that  $\alpha$  can be determined directly in the operating condition of interest. Debeau's method is well suited for high repetition rates and short pulse trains as the measurements are done in the spectral domain. On the contrary, time-domain methods such as PROUD [10] are more suited for slower repetition rates and longer pulses, provided that the photodiode has enough bandwidth. As is the case of other methods such as [10], the method outlined here is not limited to directly-modulated gain-switched lasers, but can in principle be applied to any situation in which the laser exhibits a time-periodic behaviour. Indeed, in the case of self-pulsing lasers that are not actively modulated, the RF signal at frequency  $F$  could be obtained by detecting the pulse train with a fast photodiode, followed by suitable electronic filtering and amplification. Finally, we note that the proposed method is rather accurate even when the number of frequencies in the optical spectrum is not very high, as shown in Figs. 3 and 4.

## ACKNOWLEDGMENTS

We would like to thank S. Bouhier, L. Frein for technical support and F. Bondu and G. Loas for fruitful discussions. All the numerical data treatment has been done using the Julia programming language, and the plotting using the Plots.jl package.

## DISCLOSURE

The authors declare no conflicts of interest.

## DATA AVAILABILITY

Data underlying the results presented in this paper are not publicly available at this time but may be obtained from the authors upon reasonable request.

## REFERENCES

- [1] Y. Matsui, R. Schatz, D. Che, F. Khan, M. Kwakernaak, and T. Sudo, "Low-chirp isolator-free 65-ghz-bandwidth directly modulated lasers," *Nature Photonics*, vol. 15, no. 1, pp. 59–63, 2021.
- [2] C. D. Muñoz, M. Varón, F. Destic, and A. Rissons, "Self-starting VCSEL-based optical frequency comb generator," *Optics Express*, vol. 28, no. 23, p. 34860, Nov. 2020.
- [3] B. Siquin, M. Romanelli, S. Bouhier, L. Frein, M. Alouini, and M. Vallet, "Low Phase Noise Direct-Modulation Optoelectronic Oscillator," *Journal of Lightwave Technology*, vol. 39, no. 24, pp. 7788–7793, Dec. 2021.
- [4] H. Ohta, S. Nogiwa, Y. Kawaguchi, and Y. Endo, "Measurement of 200 Gbit/s optical eye diagram by optical sampling with gain-switched optical pulse," *Electronics Letters*, vol. 36, no. 8, p. 737, 2000.
- [5] C. Henry, "Theory of the linewidth of semiconductor lasers," *IEEE Journal of Quantum Electronics*, vol. 18, no. 2, pp. 259–264, Feb. 1982.
- [6] K. Petermann, *Laser diode modulation and noise*. Springer Science & Business Media, 1991, vol. 3.
- [7] N. Opačak, F. Pilat, D. Kazakov, S. Dal Cin, G. Ramer, B. Lendl, F. Capasso, and B. Schwarz, "Spectrally resolved linewidth enhancement factor of a semiconductor frequency comb," *Optica*, vol. 8, no. 9, pp. 1227–1230, 2021.
- [8] T. Fordell and A. M. Lindberg, "Noise Correlation, Regenerative Amplification, and the Linewidth Enhancement Factor of a Vertical-Cavity Surface-Emitting Laser," *IEEE Photonics Technology Letters*, vol. 20, no. 9, pp. 667–669, May 2008.
- [9] J.-G. Provost and F. Grillot, "Measuring the Chirp and the Linewidth Enhancement Factor of Optoelectronic Devices with a Mach–Zehnder Interferometer," *IEEE Photonics Journal*, vol. 3, no. 3, pp. 476–488, Jun. 2011.
- [10] A. Consoli, B. Bonilla, J. M. G. Tijero, and I. Esquivias, "Self-validating technique for the measurement of the linewidth enhancement factor in semiconductor lasers," *Optics Express*, vol. 20, no. 5, p. 4979, Feb. 2012.
- [11] J. Debeau, B. Kowalski, and R. Boittin, "Simple method for the complete characterization of an optical pulse," *Optics Letters*, vol. 23, no. 22, p. 1784, Nov. 1998.
- [12] F. Li, Y. Park, and J. Azaña, "Complete temporal pulse characterization based on phase reconstruction using optical ultrafast differentiation (PROUD)," *Optics Letters*, vol. 32, no. 22, p. 3364, Nov. 2007.
- [13] D. A. Reid, S. G. Murdoch, and L. P. Barry, "Stepped-heterodyne optical complex spectrum analyzer," *Optics Express*, vol. 18, no. 19, p. 19724, Sep. 2010.
- [14] M. J. Connelly, J. Romero-Vivas, A. Meehan, and L. Krzczanowicz, "Dynamic power and chirp measurements of electroabsorption and Mach-Zehnder modulator pulse generators and chirp factor extraction using a linear pulse characterization technique," *Optics & Laser Technology*, vol. 121, p. 105783, Jan. 2020.
- [15] M. J. Connelly, J. Romero-Vivas, P. Morel, A. Sharaiha, F. Pommereau, and C. Fortin, "Dynamic power and chirp measurements of a quantum dash semiconductor optical amplifier amplified picosecond pulses using a linear pulse characterization technique," *Optical and Quantum Electronics*, vol. 55, no. 1, pp. 1–8, 2023.
- [16] J. Yao, "Microwave photonics," *Journal of lightwave technology*, vol. 27, no. 3, pp. 314–335, 2009.
- [17] S. Wiczorek, B. Krauskopf, T. Simpson, and D. Lenstra, "The dynamical complexity of optically injected semiconductor lasers," *Physics Reports*, vol. 416, no. 1-2, pp. 1–128, Sep. 2005.

- [18] J. Taylor, *Introduction to error analysis, the study of uncertainties in physical measurements*, 1997.
- [19] R. Tucker, "High-speed modulation of semiconductor lasers," *IEEE Transactions on Electron Devices*, vol. 32, no. 12, pp. 2572–2584, Dec. 1985.
- [20] T. Erneux and P. Glorieux, *Laser dynamics*. Cambridge University Press, 2010.
- [21] L. Chusseau, E. Hemery, and J.-M. Lourtioz, "Period doubling in directly modulated ingaasp semiconductor lasers," *Applied physics letters*, vol. 55, no. 9, pp. 822–824, 1989.